Neuron, Vol. 38, 871–885, June 19, 2003, Copyright ©2003 by Cell Press

Axon Pruning during *Drosophila* Metamorphosis: Evidence for Local Degeneration and Requirement of the Ubiquitin-Proteasome System

Ryan J. Watts,[1] Eric D. Hoopfer,[1,2] and Liqun Luo[1,2,*]
[1]Department of Biological Sciences
[2]Neurosciences Program
Stanford University
Stanford, California 94305

Summary

Axon pruning is widely used for the refinement of neural circuits in both vertebrates and invertebrates, and may also contribute to the pathogenesis of neurodegenerative diseases. However, little is known about the cellular and molecular mechanisms of axon pruning. We use the stereotyped pruning of γ neurons of the *Drosophila* mushroom bodies (MB) during metamorphosis to investigate these mechanisms. Detailed time course analyses indicate that MB axon pruning is mediated by local degeneration rather than retraction and that the disruption of the microtubule cytoskeleton precedes axon pruning. In addition, multiple lines of genetic evidence demonstrate an intrinsic role of the ubiquitin-proteasome system in axon pruning; for example, loss-of-function mutations of the ubiquitin activating enzyme (E1) or proteasome subunits in MB neurons block axon pruning. Our findings suggest that some forms of axon pruning during development may share similarities with degeneration of axons in response to injury.

Introduction

A common strategy in establishing connection specificity of the nervous system is for neurons to develop exuberant axonal and dendritic processes, followed by selective pruning of a subset of processes. For example, long-distance projection neurons from layer V of the mammalian cortex send axon branches to both the spinal cord and the superior colliculus during an early stage of development. Later in development, motor cortical neurons selectively prune their branches to the superior colliculus, whereas visual cortical neurons selectively prune their branches to the spinal cord (reviewed in O'Leary and Koester, 1993). Similarly, many insect neurons undergo specific pruning of axons and dendrites during metamorphosis, so that neurons used in the larval nervous system can be reused in the adult (reviewed in Truman, 1990).

These observations imply the existence of a program for axon self-destruction that is precisely controlled spatially and temporally. Indeed, the Otx1 transcription factor is required for the pruning of the spinal cord branch of layer V visual cortical neurons (Weimann et al., 1999). Likewise, pruning of axons and dendrites of the *Drosophila* mushroom body (MB) neurons during metamorphosis requires the cell-autonomous action of a nuclear hormone receptor complex composed of the ecdysone receptor isoform B1 (EcR-B1) and Ultraspiracle (USP), the *Drosophila* homologs of mammalian retinoic acid receptors (Lee et al., 2000a).

It is conceivable that the axon pruning machinery could be used in the adult nervous system for structural plasticity of neurons in response to learning and experience. The pruning machinery also could be used to cause atrophy of neuronal processes, a hallmark of many neurological insults including most neurodegenerative diseases (reviewed in Raff et al., 2002). However, aside from the transcriptional regulations mentioned above, little is known about the molecular machinery of the axon pruning program.

We use the pruning of *Drosophila* MB neurons during metamorphosis as a model system to investigate the cellular and molecular mechanisms of axon pruning. A single MB neuroblast sequentially generates three types of MB neurons, the γ, α′/β′, and α/β neurons, each exhibiting distinct axonal projections in adult (Lee et al., 1999). MB γ neurons, born in early larvae, initially establish a larval projection consisting of a dendritic tree and an axon peduncle, which bifurcates to give rise to a dorsal and medial branch (Figure 1A); in early pupae, MB γ neurons prune their dendrites and both the dorsal and medial axonal branches while leaving the axonal peduncle intact (Figure 1B); the medial branch then re-extends in late pupae to establish an adult-specific axon projection (Figure 1C). Interestingly, the α′/β′ neurons, born during a later larval stage, have indistinguishable axonal projections compared with γ neurons in larvae; yet, they do not prune their axons during metamorphosis, underscoring the cell type specificity of axon pruning (Lee et al., 1999).

Axon pruning could utilize one of two distinct cellular mechanisms or a combination of the two (Figure 1D). At one extreme, axons could withdraw their processes from distal to proximal, a process we term axon retraction (Figure $1D_1$). At the other extreme, axon branches to be pruned could undergo local fragmentation without large-scale retraction, a process we term local degeneration (Figure $1D_2$). In this study, we provide evidence that *Drosophila* MB γ neurons are pruned predominantly through a local degeneration mechanism. In addition, an examination of a battery of markers suggests that the disruption of the microtubule cytoskeleton precedes morphological disruption of axons.

Based on the many roles identified for the ubiquitin-proteasome system (UPS) in neurodevelopment and degeneration (reviewed in Hegde and DiAntonio, 2002), combined with our findings that axons degenerate during development, we investigated the role of the UPS in axon pruning. We provide multiple lines of genetic evidence demonstrating an essential role for the UPS in axon pruning. Our study reveals insights into the cellular and molecular mechanisms of axon pruning and suggests that some forms of developmental axon pruning may share similarities with neurodegeneration, in particular Wallerian degeneration—fragmentation of distal axons in response to axon damage.

*Correspondence: lluo@stanford.edu

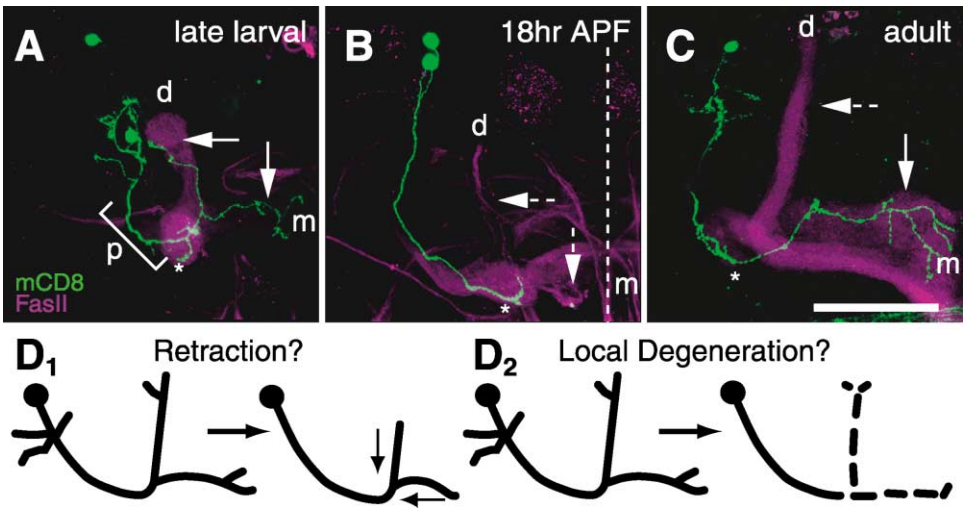

Figure 1. Axon Pruning in the *Drosophila* Mushroom Bodies

These and all subsequent images are confocal projections of the left hemisphere of the central brain, with the midline (dashed line) toward the right and dorsal up. Horizontal and vertical arrows indicate dorsal and medial branches, respectively. Asterisks signify the ends of peduncular axons and beginnings of the lobes. Scale bar equals 50 μm (except Figures 2J–2L).

(A) A γ neuron single-cell clone at a late larval stage has projections in both the dorsal (d) and medial (m) lobes.

(B) A γ neuron two-cell clone at 18 hr after puparium formation (APF) has pruned larval-specific dorsal and medial branches (dashed arrows indicate the absence of the larval branches).

(C) A γ neuron single-cell clone in adult has reextended only its medial (solid vertical arrow) but not dorsal (dashed horizontal arrow) branches.

(D) Schematic diagram of two possible cellular mechanisms of axon pruning. Retraction (D_1) is shown as branches withdraw from distal ends of the lobes, while local degeneration (D_2) is depicted by fragmentation of axons to be pruned.

Genotype: *y,w,hs-Flp,UAS-mCD8::GFP/+;FRT^{G13},UAS-mCD8::GFP,GAL4-201Y/ FRT^{G13},tubP-GAL80*. Shown as a reference, FasII staining (magenta) labels γ neurons weakly and α/β neurons strongly and does not label α′/β′ neurons.

Results

Time Course Analysis of MB γ Neuron Pruning in Single/Two-Cell Clones

To determine if axon pruning in MB γ neurons is a result of retraction or local degeneration (Figure 1D), we performed a time course analysis of pruning axons. To view axons during the remodeling process, we used the MARCM system to label one to two γ neurons per hemisphere in wild-type animals using the membrane marker mCD8::GFP (Lee and Luo, 1999). Brains from these animals were dissected and fixed every 2 hr after puparium formation (APF). This allowed for careful analysis of the morphological changes taking place during the pruning process.

The first signs of neuronal remodeling are observed at 4 hr APF when dendrites begin to appear blebbed (Figure 2B, arrowhead). At 6 hr APF, axon blebs start to appear (Figure 2C, arrows), coinciding with the removal of stereotypical larval axon terminal branches. In addition, the blebbed dendrites appear to be fragmented (Figure 2C, arrowhead). Due to their small size, it is technically difficult to analyze MB γ neuron dendrites, and therefore we mainly focus on axon structures for subsequent studies.

The appearance of strongly blebbed axons and the first signs of disconnected axon fragments are observed at the distal tips of the lobes beginning at 8 hr APF (Figure 2D, arrows). At 10 hr APF (Figures 2E and 2J–2L, arrows), we observe many axon fragments along both the dorsal and medial lobes. At higher magnification, no connections between labeled fragments are evident (Figures 2J–2L, arrows). As an example of the fragmented nature of these axons, the axon segment labeled in Figure 2L (arrowhead) is ~3.5 μm from the other fragments in the Z plane. A larger axon fragment can be observed in the 12 hr APF image (Figure 2F), in which the dorsal fragment (horizontal arrow) lies ~25 μm from the peduncle (arrowhead). However, the axonal peduncle, which also shows signs of blebbing, remains continuous throughout the pruning process (e.g., Figure 2E, arrowhead).

After 12 hr APF, axon fragments are continuously removed until very few fragments remain at 18 hr APF (Figures 2G–2I). Notably, the remaining fluorescently labeled structures tend to accumulate at the distal ends of the larval axonal branches that are pruned (Figure 2G). The time course described in Figure 2 is qualitatively similar among different animals examined ($n \geq 10$ for each time point). These data strongly support a model for local degeneration as the primary mechanism of axon pruning (Figures 1D_2 and 2M).

Changes of Cell Adhesion, Cytosolic, Synaptic, and Cytoskeletal Markers during Axon Pruning

To further analyze the sequence of events during axon pruning, we selectively express in MB γ neurons a battery of transgenes marking different cellular structures (Figure 3). In all panels shown, except Figure 3B, transgenes are expressed using the GAL4-201Y driver, which at larval and early pupal stages selectively labels γ neurons that undergo axon pruning (Lee et al., 1999). Figure 3A shows the expression of UAS-mCD8::GFP driven by GAL4-201Y in the entire population of γ neurons. The

characteristic axon pruning described in Figure 2 is recapitulated here, albeit with a lower resolution, with the onset of blebbing followed by fragmentation and removal of axon fragments in the medial and dorsal lobes.

We next examined the expression of an endogenous cell adhesion molecule, FasII, using an anti-FasII antibody (1D4; Figure 3B). FasII is expressed only in γ neurons during larval and early pupal stages. Later in pupal development, FasII is strongly expressed in newly born α/β neurons and continues to be moderately expressed in γ neurons into adulthood. Thus, FasII serves as a valuable counter stain for MB axon development (Crittenden et al., 1998; Lee et al., 1999). FasII shows colocalization with the membrane marker mCD8::GFP, revealing morphological changes characteristic of local degeneration during the pruning process (Figure 3B).

We then investigated other cellular markers in γ neurons during axon pruning by driving the expression of epitope-tagged transgenes with GAL4-201Y. We observed similar expression patterns at each time point examined for the following subcellular structures: the cytosol (GFPS65T-T10, Figure 3C), synapses (synaptotagmin::HA, Figure 3D; synaptobrevin::GFP, data not shown), and the actin cytoskeleton (GFP::Actin, Figure 3E). These experiments indicate that the detailed time course analysis performed using a membrane marker (Figure 2) does not reflect some special properties of membrane proteins. These different cellular structures appear to be turned over with a similar time course during the axon pruning process. The synaptic markers are particularly noteworthy. Their expression patterns suggest that γ neuron axons form synapses and most likely are functional during larval life (Figure $3D_1$). In addition, during the pruning process there does not appear to be a selective removal of synapses preceding the pruning of axons.

Interestingly, a myc::α-tubulin fusion protein, which serves as a marker for the microtubule cytoskeleton (Liu et al., 2000), exhibits an expression pattern during pruning that is different from all of the other examined markers. While this myc::α-tubulin is uniformly distributed in the axonal peduncles and in the dorsal and medial lobes in late larvae (Figure $3F_1$), it selectively disappears from the axons to be pruned before the loss of the actual axons (Figure 3F compared with Figure 3A, both of which are from the same animals double-labeled for mCD8::GFP and myc::α-tubulin). These results were verified with a stronger GAL4 line (OK107), suggesting that disruption of the microtubule cytoskeleton is an early step of axon pruning.

Expression of a Yeast Ubiquitin Protease Inhibits Axon Pruning

Our observation that axons undergo a destructive process during pruning led us to speculate that protein turnover may be necessary for this process. A major means of regulated protein turnover occurs via the ubiquitin-proteasome system (UPS) (Figure 4A; reviewed in Weissman, 2001). In this pathway, ubiquitin (Ub), a small peptide of 76 amino acids, is covalently linked to a substrate (S) through the activity of three enzymes. These enzymes include an ubiquitin acitivating enzyme (E1), an ubiquitin-conjugating enzyme (E2), and an ubiquitin ligase (E3). Polyubiquitinated proteins are then targeted for degradation by the 26S proteasome, which is composed of two 19S proteasome regulatory particles and the 20S core. Substrate ubiquitination may also be reversed by ubiquitin proteases (UBP).

To test the hypothesis that the UPS may play a role in axon pruning, we used GAL4-201Y to express in MB γ neurons a yeast ubiquitin protease (UBP2), which has been shown to be effective in *Drosophila* (DiAntonio et al., 2001). When examined during late larval stages, UBP2-expressing MB γ neurons exhibit largely normal growth and guidance of axons (Figure 4E compared with Figure 4B, see legend). However, at 18 hr APF, the peak of axon pruning, UBP2-expressing MB neurons fail to prune their axons (compare Figures 4F with 4C). As a consequence, γ neurons retain their dorsal lobes in the adult (Figure 4G, horizontal arrow). Thus, UBP2 expression results in specific defects in axon pruning.

Notably, we observed no effect on cell proliferation in brains expressing yeast UBP2 using either GAL4-201Y (a postmitotic driver) or GAL4-OK107 (expressed in both MB neuroblasts and neurons) (data not shown), suggesting that UBP2 does not disrupt ubiquitin-mediated cell cycle regulation. In addition, expressing a *Drosophila* UBP encoded by *fat facets* (*faf*) does not inhibit axon pruning (Table 1), suggesting a certain degree of specificity. However, since this effect on axon pruning is observed when expressing a yeast protein, we next examined whether endogenous components of the UPS in *Drosophila* are required for axon pruning.

A Genetic Requirement of *Ubiquitin activating enzyme 1* (*Uba1*) for Axon Pruning

A likely explanation for the yeast UBP2 phenotype is that expression of UBP forces substrates to be deubiquitinated, thereby reversing protein ubiquitination (Figure 4A). This model predicts that loss-of-function mutations in the enzymes that promote ubiquitination should inhibit axon pruning. To test this hypothesis, we systematically searched the *Drosophila* genome for E1, E2, and E3 enzymes and identified existing mutations either from published studies or by identifying P element insertions via "FlyBase." We then tested whether these mutants disrupt MB γ neuron pruning using the MARCM method (Figure 5A; Lee and Luo, 1999). Through this analysis, we found that a mutation in *Uba1* inhibits pruning (Figure 5); other mutants showing no observable defects in axon pruning are noted in Table 1 (see Discussion for rationale).

Uba1 encodes a predicted ubiquitin activating enzyme (E1). Our phylogenetic analysis indicates that it is the sole E1 enzyme encoded in the *Drosophila* genome (Figure 5B). UBA1 shares much stronger sequence similarities with its mammalian, worm, and yeast orthologs than with its closest related *Drosophila* protein, UBA2 (Smt3 activating enzyme 2), which is part of a SUMO (small ubiquitin-like modifier) activating enzyme complex (Donaghue et al., 2001). We identified a P element insertion that maps near *Uba1* and verified through inverse PCR that the insertion occurs in the predicted first intron between two coding exons (Figure 5C). Thus, this allele represents a loss-of-function mutation. The P element mutation was recombined onto the appropriate

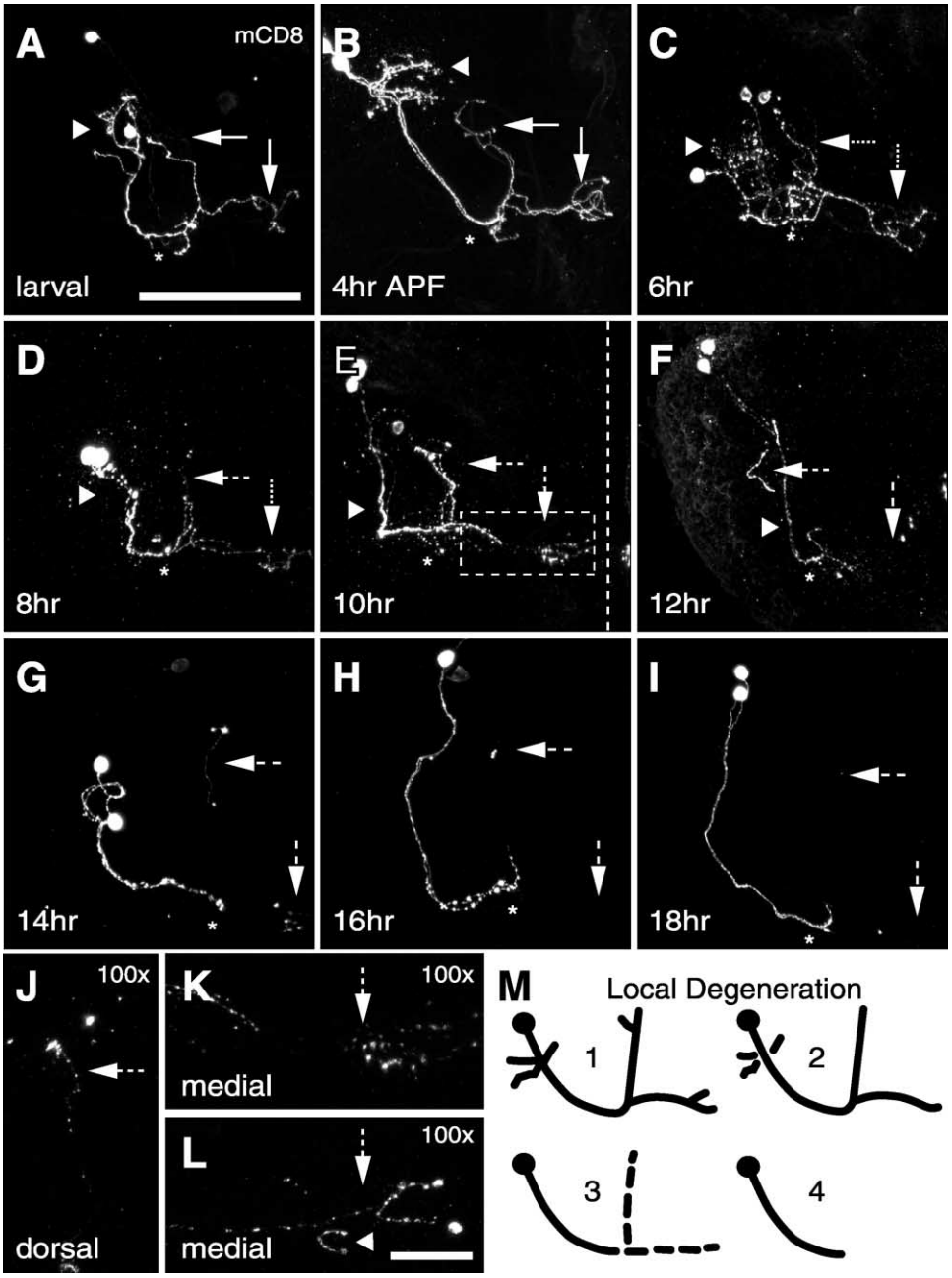

Figure 2. Time Course Analysis of MB γ Neuron Pruning

(A) Stereotypic dendrite (arrowhead) and axon (arrows) of MB γ neurons examined in late larvae.

(B) The first signs of pruning begin at 4 hr APF with the appearance of dendrite blebbing (arrowhead); the axons still appear larval-like (arrows).

(C) At 6 hr APF, both dendrites (arrowhead) and axons (arrows) appear blebbed, and fine axon terminal branches observed in larvae begin to disappear. Blebs in the dendrite region appear disconnected while axon blebs still remain continuous.

(D) At 8 hr APF, most dendrite fragments (arrowhead) have disappeared, while axons (arrows) start to appear fragmented, with mCD8-positive blebs becoming visibly disconnected.

(E) At 10 hr APF, pronounced discontinuities between blebs in the axon branch regions (arrows) are visible, while the peduncular axon (arrowhead) remains. The medial lobe (boxed) shows axon fragmentation, with localized fragments at the distal tip of the lobe and near the branch point and with a mCD8 negative gap between these regions. The box is shown at 100$\times$ magnification in (K).

(F) At 12 hr APF, many axon fragments (arrows) have disappeared; however, a large fragment (horizontal arrow) remains in the dorsal lobe, which is approximately 20–30 μm anterior (in the Z plane) of the peduncular axon (arrowhead).

(G) At 14 hr APF, an axon fragment at the distal portion of the dorsal branch is visible (horizontal arrow), and several blebs near the branching point (asterisk) and distal end of the medial branch (vertical arrow) remain.

(H) At 16 hr APF, few axon fragments remain in lobes (arrows) and tips of pruned axons near branching point still appear blebbed (asterisk).

(I) At 18 hr APF, axons are completely pruned (arrows), and the peduncular axon tip switches from a blebbed to a fine hair-like morphology (asterisk).

FRT chromosome so that positively labeled mosaic clones of *Uba1*$^{-/-}$ γ neurons could be created in an otherwise heterozygous and unstained animal using MARCM (Figures 5A and 5G–5I). Compared with wild-type neuroblast clones, neuroblast clones homozygous mutant for *Uba1* exhibit a significant reduction in the number of neurons when examined in late larvae (compare Figures 5G and 5D). This phenotype is most likely caused by an arrest of neuroblast proliferation, consistent with the notion that the UPS is essential for cell cycle progression (Weissman, 2001). The fact that *Uba1* mutant neuroblast clones can still undergo a limited number of divisions is likely due to inherited wild-type UBA1 protein from heterozygous progenitors. The growth and guidance of axons from these *Uba1*$^{-/-}$ neurons are grossly normal when examined in late larvae (Figure 5G).

Strikingly, axon pruning in *Uba1*$^{-/-}$ neurons is blocked when examined at 18 hr APF (compare Figures 5H and 5E). While nearly all axons are pruned in wild-type at this stage, *Uba1*$^{-/-}$ axons remain (arrows). As in the case of UBP2 expression (data not shown), dendrite pruning is also inhibited (Figure 5H, arrowhead). Axons that are not pruned during metamorphosis remain into adulthood (Figure 5I, arrows).

Although *Uba1*$^{-/-}$ MB neurons survive into adulthood more than 10 days after clone induction, abnormal morphology of axons, including accumulation of mCD8::GFP blebs, is clearly visible (Figure 5I, horizontal arrow). These phenotypes may reflect the pleiotropic functions of protein ubiquitination in many aspects of neuronal development and maintenance (see Discussion). However, one process that specifically requires the function of the E1 enzyme is axon pruning.

Requirement of the Proteasome for Axon Pruning

Protein ubiquitination has been shown to be used for an increasing number of cell biological processes including proteasome-mediated degradation and endocytosis (Weissman, 2001). To determine which of these ubiquitin-dependent processes is required for axon pruning, we tested mutants that disrupt the proteasome. The 19S proteasome regulatory particle is required for polyubiquitinated protein degradation; therefore, we searched for possible mutations in subunits of this complex. Our analysis of the *Drosophila* databases identified two subunits of the 19S particle with P element insertions, *Mov34* and *Rpn6*. Phylogenetic analysis of these genes strongly suggests that they are not redundant in the fly genome and are closely related to the proteasomal subunits of other organisms (Figure 6A).

The P element locations of these mutants were verified and mapped by inverse PCR (Figure 6B), predicting them to be loss-of-function mutations. These mutations were recombined onto the appropriate FRT chromosome for MARCM analysis of clonal phenotypes. As in the case with loss-of-function *Uba1*$^{-/-}$ neurons, we observed no gross defect in axon growth and guidance, but a block of axon pruning in both *Mov34*$^{-/-}$ and *Rpn6*$^{-/-}$ neurons when examined at 18 hr APF (Figures 6D and 6E compared with 6C). As a consequence of failure of axon pruning, adult clones of *Mov34*$^{-/-}$ and *Rpn6*$^{-/-}$ γ neurons also maintain their dorsal projections (Figures 6G and 6H compared with 6F).

Similarly to *Uba1*, both mutants in *Mov34* and *Rpn6* result in reduction of cell numbers in neuroblast clones, likely caused by a defect in neuroblast proliferation (Figures 6D and 6E). However, *Rpn6*$^{-/-}$ neurons, and *Mov34*$^{-/-}$ neurons to a lesser extent, show an age-dependent loss of cell number and axon projections (Figures 6G and 6H and data not shown).

The specificity of the pruning defects are best revealed in two-cell clones examined 18 hr APF. Wild-type MB γ neurons have completely pruned their dorsal and medial axonal branches and their dendrites (Figure 7A), whereas *Rpn6*$^{-/-}$ two-cell clones show intact dorsal and medial lobes as well as dendrites (Figure 7C). Similar pruning defects were also observed in two-cell clones of *Uba1*$^{-/-}$ (Figure 7B) and *Mov34*$^{-/-}$ (data not shown). Interestingly, pruning was mostly normal in single-cell clones of all three mutants (data not shown). These differences are presumably a result of differential protein perdurance; an extra cell division in two-cell clones compared with single-cell clones further dilutes the wild-type protein inherited from the heterozygous parental cell so that two-cell clones have less residual wild-type protein (Figure 5A).

We next tested whether endocytosis of target proteins, another major consequence of protein ubiquitination (monoubiquitination), is necessary for axon pruning. We generated MARCM clones homozygous for a strong loss-of-function mutation in *Clathrin heavy chain* (*Chc*) (Bazinet et al., 1993), as it is thought that monoubiquitinated proteins may undergo endocytosis via clathrin-mediated processes (Shih et al., 2002); we did not observe pruning defects in these mutants (data not shown; see Table 1). The *Drosophila shibire* (*shi*) gene encodes the dynamin GTPase essential for endocytosis (Chen et al., 1991). However, expression of a dominant-negative transgene (Moline et al., 1999), or a dominant temperature-sensitive *shibire* (*shi*) transgene at restrictive temperatures (Kitamoto, 2001), also did not inhibit axon pruning (data not shown; Table 1). These results support the notion that monoubiquitination-induced endocytosis is not required for axon pruning; rather, proteasome-mediated protein degradation after polyubiquitination is essential for axon pruning.

(J–L) 100× image at 10 hr APF of dorsal (J) or medial lobe (K and L) of degenerating axon branches showing characteristic fragments (arrows), often extremely bright and sometimes spherical in nature. No connections between fragments in distal tips and branching point regions are evident. The axon fragment labeled with arrowhead in (L) lies approximately 3.5 μm anterior from other axon fragments in the Z plane.
(M) Summary of the axon pruning process. (1) The larval morphology is characterized by dendritic branching near cell bodies and axon branches in both the dorsal and medial lobes; (2) dendrites begin to degenerate and fine axon terminal branches are lost; (3) axons begin to degenerate by fragmentation; and (4) fragments completely disappear and axon is pruned slightly past the larval branching point.
All images are confocal Z projections of single/two-cell wild-type MARCM clones (see Figure 5A) labeled with anti-mCD8. Scale bar equals 10 μm in (J) and (L).

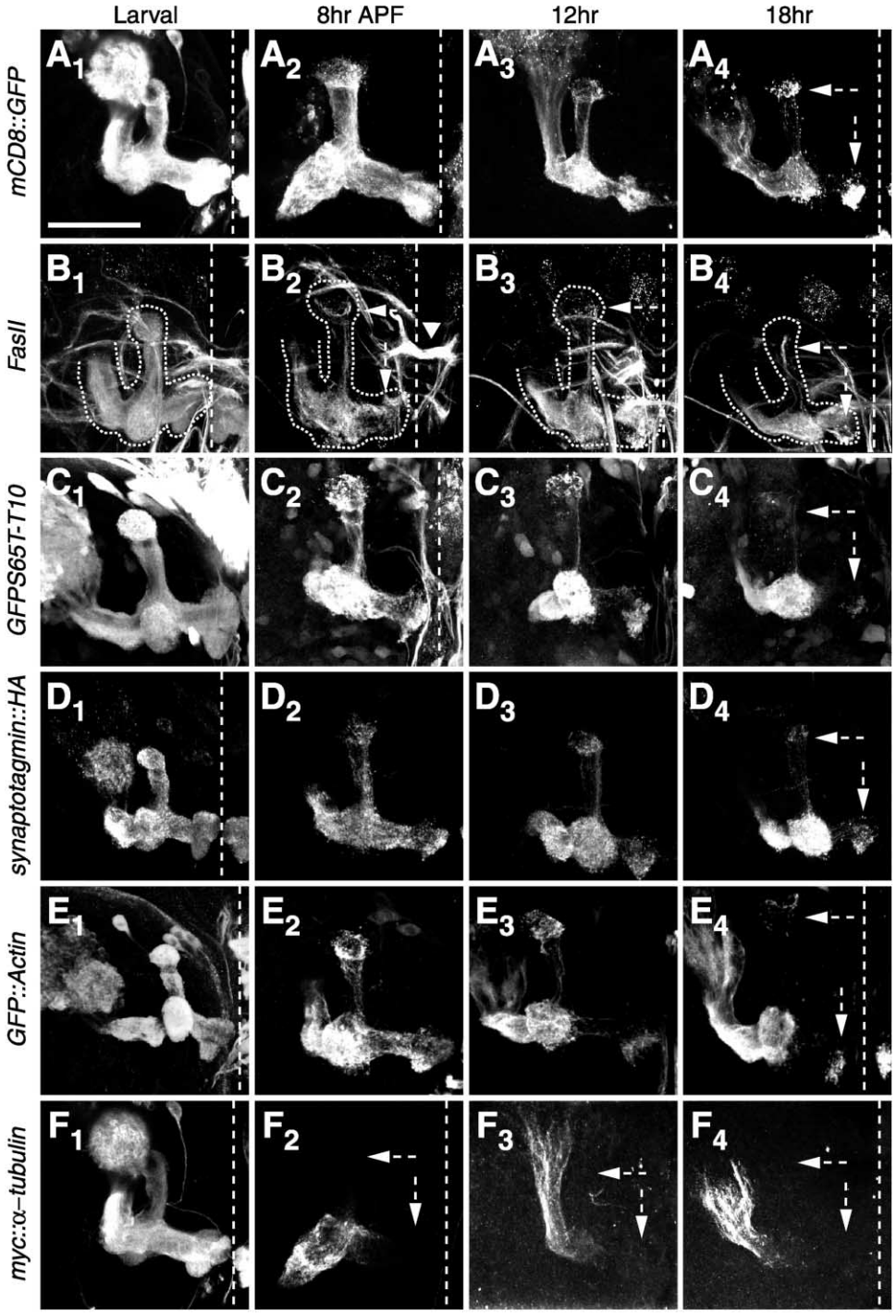

Figure 3. Characterization of Axonal Markers during MB γ Neuron Pruning

(A) Distribution of cell surface marker *mCD8::GFP* in MB γ neuron during pruning shows a progressive degeneration of axons, characterized by residual mCD8 positive axon fragments (arrows in A_4). Genotype: *UAS-mCD8::GFP,GAL4-201Y/UAS-myc::α-tubulin*.

(B) Distribution of an endogenous cell adhesion molecule, FasII, during axon pruning. FasII-positive axon fragments in MB lobes colocalize with mCD8 (channel not shown). Many other axon tracts outside the MBs are labeled with FasII during these time points (B_2, arrowhead). MBs are outlined with a dashed line for reference. Genotype: *UAS-mCD8::GFP,GAL4-201Y/+*.

(C) Distribution of cytosolic *GFPS65T-T10* during axon pruning. Distal tips of axons at 18 hr APF (arrows in C_4) are less visible relative to distal tips of mCD8 axons (arrows in A_4). Genotype: *GAL4-201Y/UAS-GFPS65T-T10*.

(D) Distribution of *Synaptotagmin::HA* during axon pruning. Staining is similar to mCD8, characterized by distal fragments staining at 18 hr APF (arrows in D_4). Genotype: *UAS-Synaptotagmin::HA/+;GAL4-201Y/+*.

(E) Expression of *Actin::GFP* during axon pruning. GFP-positive fragments are seen in the distal tips of pruning axons (arrows in E_4). Genotype: *GAL4-201Y/UAS-Actin::GFP*.

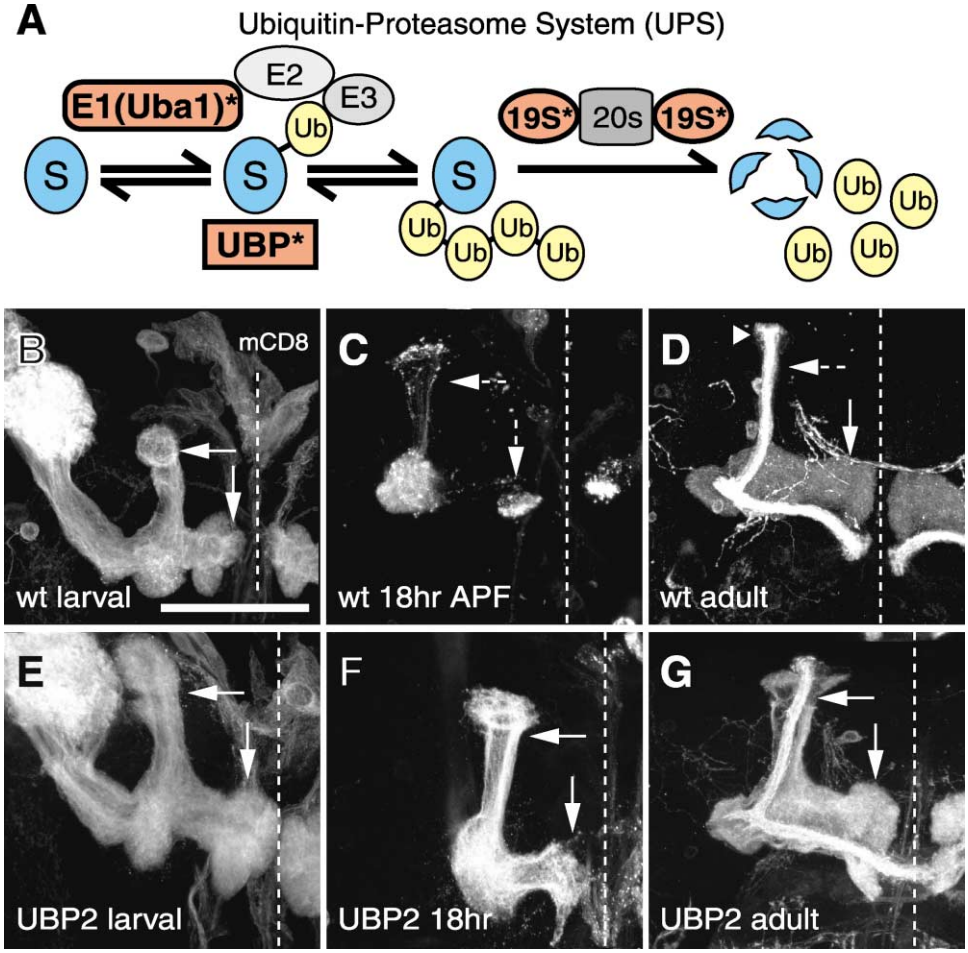

Figure 4. Expression of Yeast UBP2 in γ Neurons Inhibits Axon Pruning

(A) Diagram of the ubiquitin-proteasome system (UPS). See text for description. Orange highlights the components analyzed in this study.
(B–D) Expression of mCD8::GFP in γ neurons using GAL4-201Y representing wild-type (wt) remodeling. Note that in adult, GAL4-201Y also labels a subset of α/β neurons born in late pupae (arrowhead in D). These α/β neurons can be distinguished from the γ neurons by their projection pattern (especially in the Z plane) and staining intensity.
(E–G) Expression of UBP2 in γ neurons inhibits axon pruning. Compared to wild-type (B), UBP2-expressing larval γ neurons (E) show little overall morphological difference (arrows), except that UBP2 MBs tend to be slightly larger, likely as a result of synaptic overgrowth (DiAntonio et al., 2001). However, the larval axonal branches persist in UBP2-expressing neurons examined at 18 hr APF (F, arrows) and in adult (G, horizontal arrow).
All images are confocal Z projections visualized using anti-mCD8 labeling. n ≥ 20 brains for each time point. Genotype: *UAS-mCD8::GFP,GAL4-201Y/+* (B–D) and *UAS-mCD8::GFP,GAL4-201Y/UAS-UBP2* (E–G).

Possible Sites of Action for the UPS in the Axon Pruning Program

The UPS could act at at least three different steps in the pruning program (Figure 8A). One possibility is that it downregulates the expression of the ecdysone receptor EcR-B1 (step 1 in Figure 8A). We have previously shown that the nuclear hormone receptor complex consisting of EcR-B1 and USP is cell autonomously required for MB γ neuron pruning. In particular, while USP is ubiquitously expressed, EcR-B1 is specifically expressed in MB γ neurons but not in α′/β′ neurons that do not undergo axon pruning during metamorphosis (Lee et al., 2000a). A recent study reported that EcR-B1 transcription in MB γ neurons is regulated by the TGF-β pathway (Zheng et al., 2003). Given that the UPS is implicated in regulating TGF- β signaling (e.g., Zhu et al., 1999), it is conceivable that regulation of EcR-B1 expression is its target.

(F) Absence of *myc::α-tubulin* labeling in axon lobes prior to pruning. α-tubulin is present throughout the dendrites and axons of larval γ neurons (F_1). By 8 hr APF, α-tubulin labeling is restricted to the peduncle with no labeling in the lobes (arrows in F_2). This labeling pattern is consistent as axon pruning continues (F_3–F_4). Images for *mCD8::GFP* (A) are from the same brains as a comparison. Two different α-tubulin transgenes were tested and gave qualitatively similar results. Genotype: *UAS-mCD8::GFP,GAL4-201Y//UAS-myc::α-tubulin*.
All images are confocal Z projections of GAL4-201Y expressing transgenes (A and C–F) or endogenous FasII expression (B). ≥10 brains for each time point were examined and results are similar.

Table 1. Mutants Tested with No Obvious Pruning Defects

Gene(s)	Molecular/Cellular Function	Allele(s)	Phenotype
UbcD2	ubiquitin conjugating enzyme (E2)	k13206	moderate misguidance (6/15 NB[a])
UbcD10	ubiquitin conjugating enzyme (E2)	BG00902	severe proliferation[b] defect (4/4 NB)
cbx	ubiquitin conjugating enzyme (E2)	5704	slight prolif. defect (3/19 WB[c])
eff (UbcD1)	ubiquitin conjugating enzyme (E2)	8, s1782	moderate prolif. defect (18/19 WB, 3/6 NB)
lwr (UbcD9)	SUMO conjugating enzyme	5486	severe prolif. defect (3/3 NB)
neur[d]	ubiquitin ligase (E3)	IF65, A101	no obvious MB defect
Su(dx)	ubiquitin ligase (E3)	2	no obvious MB defect
ari-1[d]	ubiquitin ligase (E3)	EP317,[e] 2	no obvious MB defect
ari-2	ubiquitin ligase (E3)	07768	moderate prolif. defect (5/5 NB)
hiw[d]	*ubiquitin ligase (E3)*	*EMS*	*misguidance/branching (34/36 WB)*
Img	ubiquitin ligase (E3-APC complex)	03424	severe prolif. defect (15/15 NB)
lin19 (cul-1)	ubiquitin ligase complex (E3-SCF)	k01207	slight prolif. defect (7/7 NB)
slmb	ubiquitin ligase complex (E3-SCF)	00295	punctate labeling (41/41 SC[f])
faf	ubiquitin protease	EP381[e]	MB overgrowth (20/20) misguidance (14/20 WB)
grim, hid, rpr	apoptosis activators	Df(3L)H99	no obvious MB defect
p35[d]	apoptosis inhibitor	UAS-p35[e]	no obvious MB defect
Chc	vesicle coat (endocytosis)	1, 3	punctate labeling (37/37 SC)
shi[d]	dynamin GTPase (endocytosis)	K44A,[e] UAS-ts[e]	no defects (201Y) gross defects (OK107 12/12 WB)

Note: the lack of a phenotype does not constitute the ultimate proof that a specific gene listed above is not involved in axon pruning because of the following caveats: (1) a particular allele may not be a null, and (2) wild-type proteins inherited from heterozygous parent may persist for different times after clone generation.

[a] NB, neuroblast clone, mutants analyzed using MARCM.

[b] Proliferation (prolif.) refers to a reduced number of neurons in neuroblast clones. In all cases the residual neurons are early-born γ neurons, and thus the phenotype is most likely caused by a block in proliferation or death of the neuroblast.

[c] WB, whole brain, mutants analyzed are homozygous viable or transgene expression.

[d] See Experimental Procedures for fly strain information.

[e] These genes were analyzed by expression of the UAS-transgenes using either GAL4-201Y or GAL4-OK107 or both.

[f] SC, single-cell clone, mutants analyzed using MARCM.

To test this possibility, we examined expression of EcR-B1 in MB neurons expressing yeast UBP2, which inhibits axon pruning (Figure 4). We found that EcR-B1 is expressed at an apparently similar level in UBP2-expressing neurons compared with controls (Figures 8B–8D). We also examined EcR-B1 expression in MB neuroblast clones homozygous for *Uba1*. Again, EcR-B1 expression levels within and outside the clones are comparable (Figures 8E–8G). Lastly, Zheng et al. (2003) showed that forced expression of EcR-B1 in MB γ neurons could rescue pruning defects in mutants of the TGF-β signaling pathway. However, we found that forced expression of EcR-B1 could not rescue the pruning failure phenotype in UBP2-expressing neurons (data not shown). Taken together, these experiments rule out the possibility that the UPS acts primarily by regulating EcR-B1 expression and suggest that it acts either at the initiation or execution steps of the pruning process (Figure 8A, steps 2 and 3, respectively; see Discussion).

Discussion

Cellular Mechanisms of Axon Pruning

Although axon pruning has been widely reported in the construction of the vertebrate and invertebrate nervous systems, the cellular mechanisms underlying axon pruning have been reported in only few cases. In the formation of the vertebrate neuromuscular junction, the initial pattern of multiple innervation (one motor neuron innervating multiple muscle fibers) is later converted to a single innervation pattern (one motor neuron innervating one muscle fiber) through elimination of extra branches (reviewed in Sanes and Lichtman, 1999). Time-lapse microscopic imaging suggests that retraction is the primary mode for pruning of motor axon terminals (Bernstein and Lichtman, 1999; Walsh and Lichtman, 2003). As a second example, in the establishment of retinotectal map of the vertebrate visual system, axons of retinal ganglion cells tend to overshoot their final targets. Nakamura and O'Leary (1989) observed fragments of DiI-labeled axons in the overshooting region, suggesting that degeneration could be involved in pruning axons to their final target. In most other cases, the cellular mechanisms have not been reported. Both modes of axon pruning have their advantages. For instance, axon retraction allows more complete recovery of materials within the pruned axons. Local degeneration allows more efficient removal of unwanted axons and disconnection with their potential synaptic targets. Different mechanisms might be utilized in achieving these two modes of axon pruning.

In this study, we present evidence for local degeneration as the predominant cellular mechanism for axon pruning in MB neurons (Figures 2 and 3). By examining large numbers of single/two-cell clones of γ neurons every 2 hr during early metamorphosis (0–18 hr APF), we observed a stereotyped pruning process starting from blebbing of dendrites and dendritic pruning, followed by blebbing in axons and disintegration into discretely labeled spots (Figure 2M). Importantly, we never observed intact axons retracting from distal ends. In contrast, fragments of axons along the path are often observed with a peak frequency at 10–12 hr APF. In fact, the most distal ends of larval branches persist the longest. We have attempted to image the pruning process in live samples. However, due to the depth of

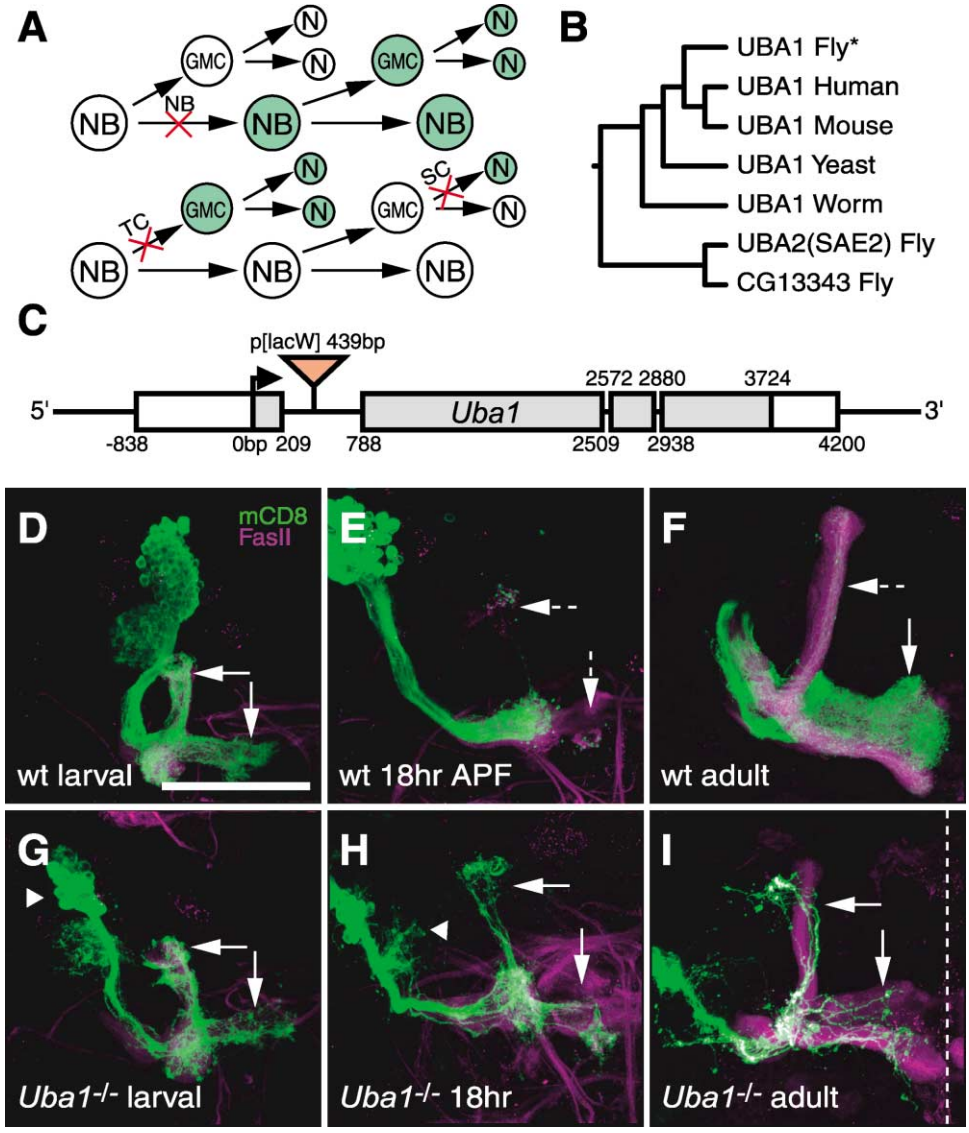

Figure 5. Mutation in *Uba1* Inhibits Axon Pruning

(A) Schematic of possible MARCM clone types generated in the mushroom bodies (Lee et al., 1999). Abbreviations: NB, neuroblast clone that labels the neuroblast (NB) and all subsequent progeny when induced during neuroblast division; TC, two-cell clone that labels the ganglion mother cell (GMC) and subsequent progeny, two neurons, when induced during neuroblast division; SC, single-cell clone that labels a single neuron (N) when mitotic recombination is induced during ganglion mother cell division.

(B) Dendrogram of proteins related to *Drosophila* UBA1. Analysis was performed using Clustal W (http://clustalw.genome.ad.jp/) of related proteins identified by BlastP (http://www.ncbi.nlm.nih.gov/blast).

(C) Schematic diagram of P element insertion in *Uba1* showing insertion site relative to predicted exon/intron map. 0 bp indicates the start of the open reading frame (in gray). Another putative translation start site lies at −549 bp.

(D–F) Wild-type neuroblast clones showing characteristic pruning of γ neuron larval branches (arrows in D) at 18 hr APF (dashed arrows in E) and absence of dorsal branches in adult (dashed arrow in F).

(G–I) *Uba1*$^{-/-}$ neuroblast clones show grossly normal larval axonal projections to both the dorsal and medial lobes (arrows in G); however, there are fewer cells in *Uba1*$^{-/-}$ clones (arrowhead in G) as compared to wild-type. Pruning defects are evident at 18 hr APF, indicated by the persistence of continuous larval branches (arrows in H). Dendrite pruning is also inhibited in *Uba1*$^{-/-}$ clones (arrowhead in H). Axons that fail to prune in *Uba1*$^{-/-}$ NB clones remain in the adult and can be identified by FasII-positive expression and orientation relative to the α/β lobe labeled with anti-FasII (arrows in I).

All images are confocal Z projections and are double-labeled with anti-mCD8 for MARCM clones (green) and FasII (magenta). Genotype: *y,w,hs-Flp,UAS-mCD8::GFP/+;FRT*^{G13}*,UAS-mCD8::GFP,GAL4-201Y/ FRT*^{G13}*,tubP-GAL80* (D–F), *y,w,hs-Flp,UAS-mCD8::GFP/+;FRT*^{G13}*,Uba1*^{s3484}*,UAS-mCD8::GFP,GAL4-201Y/ FRT*^{G13}*,tubP-GAL80* (G–I). n ≥ 10 NB clones for each time point.

the brain inside the pupal case and the presence of opaque tissues surrounding the brain, we could not image MB axons using confocal or two-photon microscopy in intact animals. We also could not faithfully recapitulate the pruning process in cultured brain in the presence of the metamorphic hormone ecdysone (data

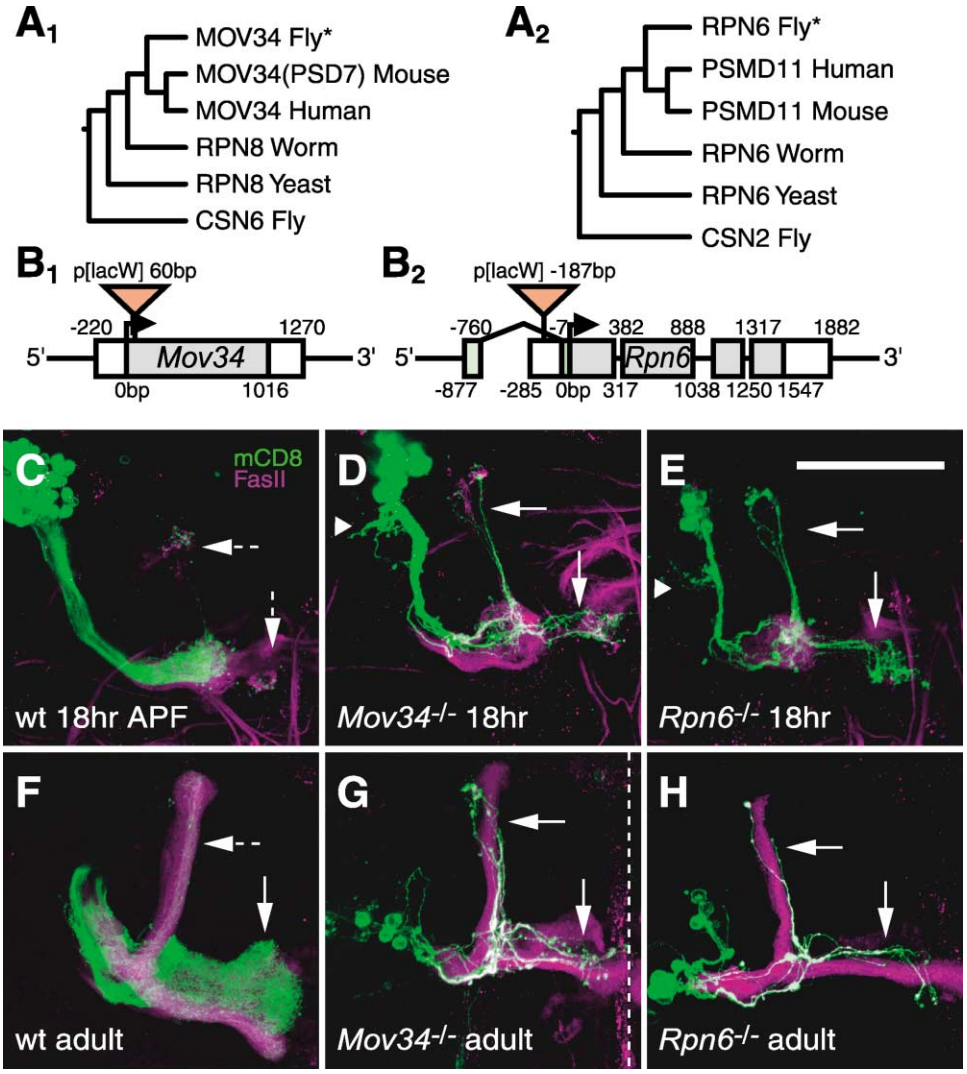

Figure 6. Mutations in 19S Proteasome Regulatory Particle Subunits, *Mov34* and *Rpn6*, Inhibit Axon Pruning

(A) Dendrograms of proteins related to Mov34 (A_1) and Rpn6 (A_2). Analysis was performed as described in Figure 5.

(B) Schematic diagram of P element insertions in *Mov34* (B_1) and *Rpn6* (B_2) showing insertion sites relative to exon/intron map. 0 bp indicates the start of the open reading frame (in gray). Green exons in *Rpn6* (B_2) represent alternative splicing or two separate promoters (two possible first exons as determined by cDNA sequence).

(C and F) Wild-type NB clones in 18 hr APF (C) or adult (F) show characteristic pruning of γ neurons.

(D and G) *Mov34*$^{-/-}$ NB clones in 18 hr APF (D) or adult (G) show inhibition of γ neuron pruning.

(E and H) *Rpn6*$^{-/-}$ NB clones in 18 hr APF (E) or adult (H) show inhibition of γ neuron pruning.

Imaging and labeling are as in Figure 5. Genotype: (C) and (F) as described for wt in Figure 5; *y,w,hs-Flp,UAS-mCD8::GFP/+;FRT*^{G13}*,UAS-mCD8::GFP,GAL4-201Y, Mov34*^{k08003}*/ FRT*^{G13}*,tubP-GAL80* (D and G) *y,w,hs-Flp,UAS-mCD8::GFP/+;FRT*^{G13}*,Rpn6*^{k00103}*,UAS-mCD8::GFP,GAL4-201Y/ FRT*^{G13}*,tubP-GAL80* (E and H). n ≥ 10 clones for each time point.

not shown). Despite the lack of live imaging data, this detailed time course analysis of fixed samples argues strongly that fragmentation of axons along their length (local degeneration) is the predominant mechanism for MB axon pruning.

This does not, however, mean that these MB axons are incapable of retraction. We have previously described a potent axon retraction pathway in MB neurons. Axon retraction can be caused by activation of small GTPase RhoA, signaling through its downstream effector kinase Drok, which phosphorylates the myosin regulatory subunit, eventually activating myosin II-mediated actomyosin contractility. This pathway is normally inactive due to the negative regulation of RhoA activity by p190 RhoGAP. Bypassing p190 RhoGAP negative regulation through RNAi inhibition of p190, expression of constitutively active RhoA or Drok both result in MB axon retraction (Billuart et al., 2001). However, the MB γ neuron pruning described in this study is distinct from RhoA-mediated axon retraction, as null mutations in *RhoA*, *Drok,* or *spaghetti squash* (which encodes the myosin regulatory light chain) do not inhibit MB γ neuron pruning during metamorphosis (Billuart et al., 2001; Lee et al., 2000b; Winter et al., 2001). Moreover, MB γ neuron pruning described here is a natural event that occurs only during early metamorphosis. In contrast, RhoA-dependent axon retraction, at least to a comparable level (removal of an entire lobe), occurs only when this pathway

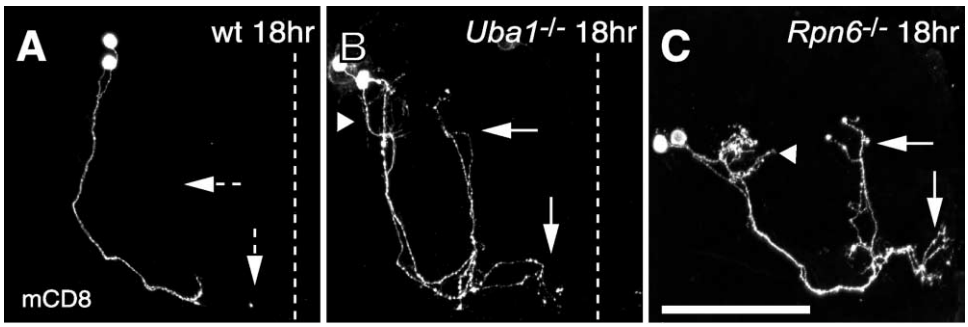

Figure 7. Two-Cell Clone Analysis

Compared with wild-type two-cell clones showing characteristic pruning of γ neurons at 18 hr APF (A), two-cell clones of *Uba1*$^{-/-}$ (B) or *Rpn6*$^{-/-}$ (C) fail to prune their larval-specific dorsal and medial branches (horizontal and vertical arrows) as well as their dendrites (arrowheads). Genotypes are as in Figures 5 and 6, and labeling is the same as in Figure 2. n ≥ 8 clones for each time point.

is abnormally activated; it can occur at any time during pupal life and even in adult (Billuart et al., 2001). Thus, MB γ neuron pruning described here and RhoA-mediated axon retraction are two entirely different processes developmentally, cell biologically, and mechanistically.

To explore the sequence of events in axon pruning,

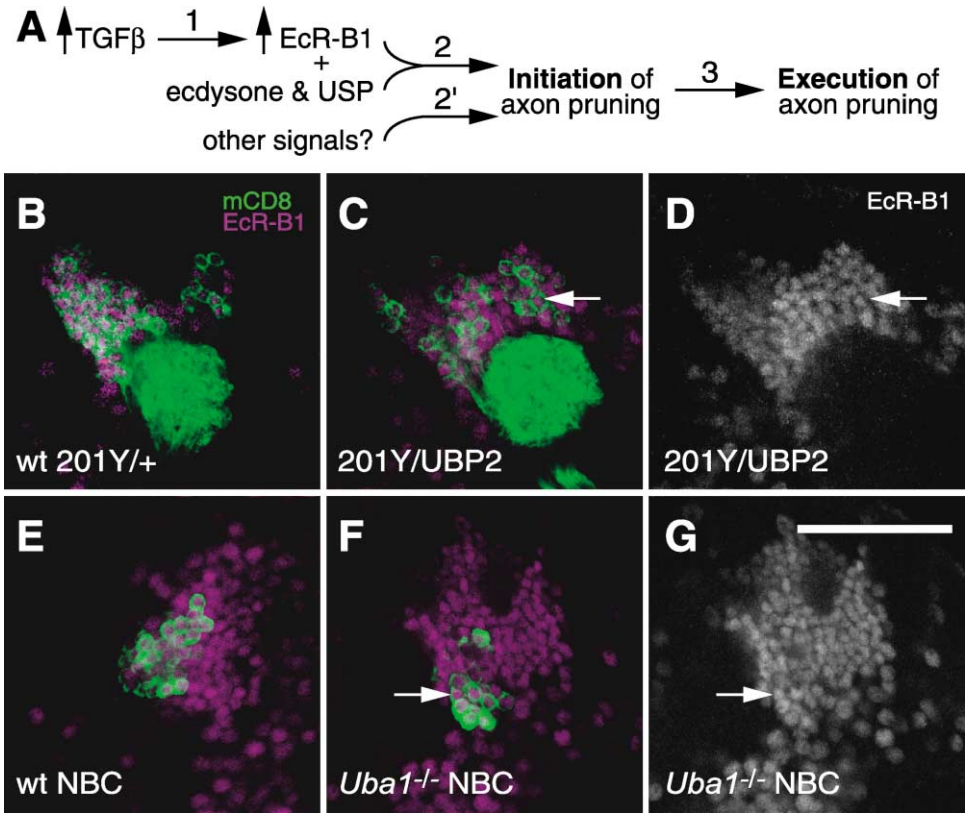

Figure 8. EcR-B1 Expression Is Unaltered in Ubiquitin-Proteasome Mutants

(A) Schematic of possible sites of action of the UPS. See text for details.

(B) Expression of endogenous EcR-B1 in MB expressing UAS-mCD8::GFP driven by GAL4-201Y.

(C and D) Coexpression of UAS-UBP2 and UAS-mCD8::GFP (green) driven by GAL4-201Y shows no noticeable difference of EcR-B1 expression (magenta) as compared to wt (B). EcR-B1 channel alone is shown in (D).

(E) Expression of endogenous EcR-B1 (magenta) in wild-type (wt) neuroblast (NB) clone (green).

(F and G) The level of endogenous expression of EcR-B1 (magenta) is similar within (arrow) or outside a *Uba1*$^{-/-}$ neuroblast clone (NBC, marked by green). EcR-B1 expression alone in a *Uba1*$^{-/-}$ NBC is shown in (G).

All images are single confocal sections. Brains were double-labeled with anti-mCD8 (green) and anti-EcR-B1 (magenta) from late third instar larvae and imaged under identical conditions. Genotype: *UAS-mCD8::GFP,GAL4-201Y/+* (B); *UAS-mCD8::GFP,GAL4-201Y/UAS-UBP2* (C and D); *y,w,hs-Flp,UAS-mCD8::GFP/+;FRT*^{G13}*,UAS-mCD8::GFP,GAL4-201Y/ FRT*^{G13}*,tubP-GAL80* (E); and *y,w,hs-Flp,UAS-mCD8::GFP/+;FRT*^{G13}*, UAS-mCD8::GFP,GAL4-201Y, Uba1*^{s3484}*/ FRT*^{G13}*,tubP-GAL80* (F and G). n ≥ 15 brains (B–D) and n ≥ 5 NB clones (E–G).

we also examined markers for different subcellular structures in addition to the mCD8::GFP cell surface marker (Figure 3). Interestingly, whereas all other markers show a time course of distribution similar to that of mCD8::GFP, an epitope-tagged tubulin marker is absent at earlier time points in the axon lobes destined to be pruned, suggesting that disruption of the microtubule cytoskeleton is one of the first steps of axon pruning. Our preliminary observations using electron microscopy confirm this interpretation (R.J.W., C. Larsen, J. Perrino, and L.L., unpublished data).

An intriguing aspect of axon pruning is its striking spatial precision. In the same MB neurons, axons are only pruned to a specific point: the medial and dorsal branches are completely pruned, whereas the peduncular section of the axons remains. We do not know how this subcellular specificity is achieved; however, our time course analysis provides some insight. We found that blebs are not restricted to the axons to be pruned; they are also distributed along the peduncular axons. Thus, one possible scenario is that a systemic signal from the nucleus (for instance, controlled by EcR-B1/USP-mediated transcription) instructs the neurons to enter a state competent for pruning, which may include the formation of blebs. Then an external signal provides the spatial cue along the portions of the axons to be pruned. Another possibility is that the spatial selectivity is achieved by a single cut separating the axons to be pruned from those to be preserved; distal axons then undergo fragmentation as a secondary consequence.

Molecular Mechanisms of Axon Pruning

Prior to our study, proteins known to regulate axon pruning were limited to transcription factors and their upstream regulators (Lee et al., 2000a; Weimann et al., 1999; Zheng et al., 2003), implying the existence of a genetic program regulating axon pruning. A recent study identified semaphorin as an extracellular inducer for stereotyped pruning of hippocampal axon branches (Bagri et al., 2003). We provide several lines of genetic evidence that the UPS plays an intrinsic role in MB neurons for axon pruning. First, expression of a yeast ubiquitin protease, which removes ubiquitin from substrates and could reverse UPS-mediated protein degradation (DiAntonio et al., 2001), potently inhibits axon pruning (Figure 4). The specificity of this experiment is highlighted by the fact that no pruning phenotypes were observed when we examined expression of ~1000 random *Drosophila* genes through an "EP" screen (Rorth, 1996) using the same driver, GAL4-201Y, or an even stronger MB driver, GAL4-OK107 (R.J.W., S. Marticke, and L.L., unpublished results). Second, MB γ neurons homozygous for a loss-of-function allele of *Uba1*, encoding the apparent single-copy ubiquitin activating enzyme (E1), exhibit strong pruning defects (Figures 5 and 7B). Third, MB γ neurons homozygous for loss-of-function alleles of two proteasome subunits exhibit pruning phenotypes analogous to loss of E1 (Figures 6 and 7C), indicating that proteasome-mediated protein degradation accounts for the requirement of protein ubiquitination during axon pruning. In these genetic experiments, a theoretical possibility exists that background mutation(s) on the same chromosome arm contributes to observed phenotypes. However, given that mutations in three components of the UPS give virtually identical axon pruning phenotypes, this possibility is extremely unlikely. To definitively control for this remote possibility would require excising the mutagenic P elements, which for technical reasons we were not able to perform (see Experimental Procedures).

Although we ruled out the possibility that the UPS acts upstream of EcR-B1 transcriptional regulation (Figure 8), we do not currently have definitive evidence to distinguish between the following two broad possibilities (Figure 8A, steps 2 and 3). The UPS could act at the initiation step of axon pruning, by degrading one or more negative regulators of the pruning machinery. This regulation could be downstream of (step 2), or in parallel (step 2′) with, EcR-B1/USP transcriptional regulation. Alternatively, the UPS could act at the execution step (step 3) by degrading many proteins, for example structural proteins, thus facilitating the actual process of axon pruning. We favor the "initiation" model over the "execution" model, because fine structure analysis of mutant two-cell clones for E1 or proteasome subunits reveals an almost complete block of axon pruning (Figure 7); one would predict that if the UPS is used in the execution step, a partial pruning phenotype might result.

The UPS is widely utilized in nervous system development and function, including axon guidance, synapse development, maturation, and plasticity (Hegde and DiAntonio, 2002). Here we identify a new role for this versatile system—regulation of axon pruning. The specificity of this system in regulating so many processes may rely on the sizable number of ubiquitin conjugating enzymes (E2s), and particularly ubiquitin ligases (E3s) found in the genome. We have found at least 30 E2s and 50 E3s in the *Drosophila* genome; most certainly this is an underestimate. We tested 4 E2s and 8 E3s with existing mutants and found that none of them block axon pruning (Table 1). Most likely this is because we have not found the E2/E3(s) responsible for axon pruning, whereas perturbing the activity of the single E1 (Uba1) or proteasome subunits blocks the entire UPS. Future identification of specific E2/E3(s) and the substrate(s) essential for axon pruning will further elucidate the machinery of axon pruning and its regulation; it may also provide a definitive distinction between the initiation and the execution models.

Potential Similarity of MB Axon Pruning and Wallerian Degeneration

When an axon is cut, the distal portion undergoes characteristic fragmentation and degeneration, a process termed "Wallerian degeneration" (Waller, 1850; Raff et al., 2002). The resemblance of MB axon pruning described here to Wallerian degeneration raises the possibility that they may utilize similar molecular mechanisms.

Since Wallerian degeneration involves degradation of cellular structures in a manner that resembles apoptosis, the involvement of caspases has been systematically investigated in a previous study (Finn et al., 2000). It was found that caspase inhibitors, while effective in preventing neuronal death in response to axon severing, do not affect Wallerian degeneration of distal axons. We provide two lines of evidence that MB axon pruning does

not utilize the apoptosis machinery. First, we tested the *H99* deletion, which removes three apoptosis activators in *Drosophila* (*grim*, *hid*, *rpr*); homozygosity of this deletion blocks apoptosis in many developmental processes examined (Chen et al., 1996; Grether et al., 1995; White et al., 1994). However, we found that axon pruning is normal in MB neuroblast clones homozygous for the *H99* deletion (Table 1; data not shown). Second, viral protein p35, acting as a caspase inhibitor, has been shown to block apoptosis when expressed in *Drosophila* (Hay et al., 1994). When the UAS-p35 transgene was expressed in MB neurons, we did not observe any defects in axon pruning (Table 1). Thus, similar to Wallerian degeneration, MB axon pruning does not appear to utilize the caspase-dependent apoptosis machinery.

While the molecular mechanisms of Wallerian degeneration are largely unknown, the mutant mouse *Wallerian degeneration slow* (*Wld*^{s}) provides some interesting insights. In *Wld*^{s} mice, degeneration of distal axons in response to cutting is greatly slowed (Glass et al., 1993; Perry et al., 1990). The *Wld*^{s} mutation results in expression of a fusion protein consisting of the N-terminal 70 amino acids of UFD2/E4, an evolutionarily conserved protein used in protein polyubiquitination (Koegl et al., 1999), and the nicotinamide mononucleotide adenylyltransferase (Nmnat) (Conforti et al., 2000). Transgenic expression of the fusion protein protects distal axon degeneration in a dose-dependent fashion (Mack et al., 2001). Thus, it has been suggested that perturbation of the UPS serves as a protective mechanism for Wallerian degeneration in *Wld*^{s} mice (Coleman and Perry, 2002). Additionally, inhibition of the UPS in a Wallerian degeneration paradigm delays axon fragmentation (Zhigang He, personal communication). Our finding of a genetic requirement for the UPS in MB axon pruning provides another line of evidence for the similarities between a developmentally regulated process of axon pruning and a pathological process of axon degeneration in response to injury.

Implications for the Involvement of the UPS in Neurodegenerative Diseases

The UPS has been implicated in many neurodegenerative diseases including Alzheimer's, Parkinson's, and poly-glutamine repeat diseases, a common feature of which is the abnormal accumulation of proteins (reviewed in Miller and Wilson, 2003). Inhibition of the UPS may enhance the abnormal accumulation of proteins, which could in turn further impair the system (e.g., Bence et al., 2001). Indeed, several neurodegenerative diseases are caused by genetic mutations that likely inhibit the UPS (Miller and Wilson, 2003). Thus, a therapeutic strategy for these neurodegenerative diseases could be to enhance ubiquitin-proteasome activity.

Our findings complicate this strategy. While long-term deprivation of E1 or proteasome subunits results in abnormal neuronal morphology or neuronal death (Figures 5 and 6), indicating that the UPS is required to maintain neuronal health, we also found a positive role for the UPS in the initiation or execution of axon pruning through a degenerative mechanism. Thus, enhancing the UPS could lead to aberrant activation of axon pruning. On the other hand, inhibiting the UPS could prevent acute axon degeneration, yet would be detrimental to long-term neuronal health. One solution to this paradox is to identify E2/E3(s) specific for axon pruning, thus providing potential targets for preventing axon degeneration.

Experimental Procedures

Fly Strains

The majority of the mutants analyzed in this study were obtained from the Bloomington stock center (http://flystocks.bio.indiana.edu/) and were identified through "Flybase" (http://flybase.bio.indiana.edu/). The alleles with pruning defects created by P element insertions in genes are *Uba1*^{s3484}, *Mov34*^{k08003}, and *Rpn6*^{k00103}. Other lines used in this study include UAS-UBP2 (DiAntonio et al., 2001), *FRT82B, neur*$^{IF65\ \&\ A101}$ (Lai et al., 2001), *ari-1*^{2} (Aguilera et al., 2000), *hiw*^{EMS} (Wan et al., 2000), UAS-p35 (Hay et al., 1994), and UAS-*shi*^{ts1} (Kitamoto, 2001).

Clonal Analysis of MB γ Neurons

To generate MARCM clones in γ neurons, embryos were collected over an 8 hr time window and aged for 24 hr at 25°C. Newly hatched larvae were heat-shocked at 37°C for 1 hr. Brains were then dissected at various stages. For time course analysis, white pupae were picked every 2 hr (0–2 hr APF) and aged at 25°C until the appropriate time for dissection. Candidate gene analysis consisted of recombining mutations onto the appropriate FRT chromosome and generating MARCM clones as described above.

For clonal analysis of *Uba1*, *Mov34*, or *Rpn6*, we did not perform P element excisions to revert the phenotype because of technical difficulty: at least two additional P elements must be on the same 2R chromosomal arm (FRT^{G13} and GAL4-201Y) for phenotypic analysis. The fact that mutations in these three separate genes in the UPS gave almost identical pruning phenotypes makes it extremely unlikely that the pruning phenotypes are caused by background mutations. The following data provide additional support. (1) We first recombined these P elements with FRT^{G13} and the recombination rates are consistent with the notion that the phenotypes are caused by the P elements. *Uba1*: predicted based on genetic map position, 3.3%, observed, 3.75% (3/80); *Rpn6*: predicted, 16.7%, observed, 10% (3/30); *Mov34*: predicted, 50%, observed, 42.9% (6/14). (2) All three mutants were then recombined with *UAS-mCD8::GFP,Gal4-201Y* to specifically label γ neurons. For *Uba1* and *Rpn6* this recombination resulted in removal of the majority of the distal portion of original P element chromosome. For *Mov34*, which lies distal to Gal4-201Y, the majority of the proximal portion of the original P element chromosome was removed when recombined. Recombination frequencies observed for these crosses were also as predicted. Both lethality and presence of P element always accompanied pruning defects.

In all examples of wild-type and mutant clones shown in this study, we used the GAL4-201Y driver to express UAS-mCD8::GFP, a membrane marker, and used tubP-GAL80 to repress the expression of this membrane marker in nonclonal cells (Lee and Luo, 1999). This ensured that all MB neurons viewed before late pupal stages were γ neurons.

Transgene Expression

The GAL4-201Y driver was used for all transgene expression experiments. In the cases of UAS-UBP2, UAS-synaptotagmin::HA, and UAS-myc::αtubulin, the membrane marker UAS-mCD8::GFP was coexpressed with these trangenes. In several other cases, we coexpressed UAS-CD2, another membrane marker (data not shown). Pupae were aged and dissected at appropriate times as described in the previous section.

Inverse PCR

To identify the location of inserted P elements, inverse PCR was performed as described (http://www.fruitfly.org/about/methods/inverse.pcr.html). Flanking sequence was "Blasted" against the *Drosophila* genome to identify the exact nucleotide insertion site. Exon/intron maps and the relative positions of P element insertions were created by comparing sequenced or predicted cDNAs with published genomic sequence.

Immunohistochemistry

Brains were dissected, fixed, and processed as previously described (Lee et al., 1999; Lee and Luo, 1999). Antibodies used in this study include: rat monoclonal anti-mouse CD8 α subunit, 1:100 (Caltag); mouse monoclonal 1D4, 1:100 (anti-FasII, gift of C. Goodman); mouse monoclonal AD4.4, 1:20 (anti-EcR-B1; Talbot et al., 1993); rabbit anti-GFP, 1:500 (Molecular Probes); mouse monoclonal anti-c-Myc (9E10), 1:50 (Santa Cruz Biotechnology); mouse monoclonal anti-HA.11, 1:1000 (Babco); Alexa-488 conjugated goat anti-rat IgG 1:400; Alexa-568 conjugated goat anti-mouse IgG, 1:400 (Molecular Probes); and FITC-conjugated goat anti-rabbit IgG, 1:100 (Jackson). Images were collected using a Bio-Rad MRC 1024 laser-scanning confocal microscope and Laser Sharp image-collection software, then processed using ImageJ (http://rsb.info.nih.gov/ij/) and Adobe Photoshop.

Acknowledgments

We thank A. DiAntonio, B. Hay, T. Kitamoto, E. Lai, A. Ferrús, B. Zhang, and the Bloomington Stock Center for mutants and transgenes. We thank Zhigang He for communicating results prior to publication. We thank discussions and critical comments of our manuscript from members of the Luo lab and B. Barres, R. Kopito, S. McConnell, M. Raff, M. Simon, and M. Tessier-Lavigne. We also thank E. Gomez and C. Wheeler for their experimental help. This work was supported by an NIH grant (R01-NS41044).

Received: March 6, 2003
Revised: April 11, 2003
Accepted: April 14, 2003
Published: June 18, 2003

References

Aguilera, M., Oliveros, M., Martinez-Padron, M., Barbas, J.A., and Ferrus, A. (2000). Ariadne-1: a vital *Drosophila* gene is required in development and defines a new conserved family of ring-finger proteins. Genetics *155*, 1231–1244.

Bagri, A., Cheng, H.-J., Yaron, A., Stein, E., Pleasure, S.J., and Tessier-Lavigne, M. (2003). Stereotyped pruning of long hippocampal axon branches triggered by retraction inducers of the Semaphorin family. Cell *113*, 285–299.

Bazinet, C., Katzen, A.L., Morgan, M., Mahowald, A.P., and Lemmon, S.K. (1993). The *Drosophila* clathrin heavy chain gene: clathrin function is essential in a multicellular organism. Genetics *134*, 1119–1134.

Bence, N.F., Sampat, R.M., and Kopito, R.R. (2001). Impairment of the ubiquitin-proteasome system by protein aggregation. Science *292*, 1552–1555.

Bernstein, M., and Lichtman, J.W. (1999). Axonal atrophy: the retraction reaction. Curr. Opin. Neurobiol. *9*, 364–370.

Billuart, P., Winter, C.G., Maresh, A., Zhao, X., and Luo, L. (2001). Regulating axon branch stability: the role of p190 RhoGAP in repressing a retraction signaling pathway. Cell *107*, 195–207.

Chen, M.S., Obar, R.A., Schroeder, C.C., Austin, T.W., Poodry, C.A., Wadsworth, S.C., and Vallee, R.B. (1991). Multiple forms of dynamin are encoded by shibire, a *Drosophila* gene involved in endocytosis. Nature *351*, 583–586.

Chen, P., Nordstrom, W., Gish, B., and Abrams, J.M. (1996). grim, a novel cell death gene in *Drosophila*. Genes Dev. *10*, 1773–1782.

Coleman, M., and Perry, V. (2002). Axon pathology in neurological disease: a neglected therapeutic target. Trends Neurosci. *25*, 532–537.

Conforti, L., Tarlton, A., Mack, T.G., Mi, W., Buckmaster, E.A., Wagner, D., Perry, V.H., and Coleman, M.P. (2000). A Ufd2/D4Cole1e chimeric protein and overexpression of Rbp7 in the slow Wallerian degeneration (WldS) mouse. Proc. Natl. Acad. Sci. USA *97*, 11377–11382.

Crittenden, J.R., Sloulakis, E.M.C., Han, K.-A., Kalderon, D., and Davis, R.L. (1998). Tripartite mushroom body architecture revealed by antigenic markers. Learn. Mem. *5*, 38–51.

DiAntonio, A., Haghighi, A.P., Portman, S.L., Lee, J.D., Amaranto, A.M., and Goodman, C.S. (2001). Ubiquitination-dependent mechanisms regulate synaptic growth and function. Nature *412*, 449–452.

Donaghue, C., Bates, H., and Cotterill, S. (2001). Identification and characterisation of the *Drosophila* homologue of the yeast Uba2 gene. Biochim. Biophys. Acta *1518*, 210–214.

Finn, J.T., Weil, M., Archer, F., Siman, R., Srinivasan, A., and Raff, M.C. (2000). Evidence that wallerian degeneration and localized axon degeneration induced by local neurotrophin deprivation do not involve caspases. J. Neurosci. *20*, 1333–1341.

Glass, J.D., Brushart, T.M., George, E.B., and Griffin, J.W. (1993). Prolonged survival of transected nerve fibres in C57BL/Ola mice is an intrinsic characteristic of the axon. J. Neurocytol. *22*, 311–321.

Grether, M.E., Abrams, J.M., Agapite, J., White, K., and Steller, H. (1995). The head involution defective gene of *Drosophila melanogaster* functions in programmed cell death. Genes Dev. *9*, 1694–1708.

Hay, B.A., Wolff, T., and Rubin, G.M. (1994). Expression of baculovirus P35 prevents cell death in *Drosophila*. Development *120*, 2121–2129.

Hegde, A.N., and DiAntonio, A. (2002). Ubiquitin and the synapse. Nat. Rev. Neurosci. *3*, 854–861.

Kitamoto, T. (2001). Conditional modification of behavior in *Drosophila* by targeted expression of a temperature-sensitive shibire allele in defined neurons. J. Neurobiol. *47*, 81–92.

Koegl, M., Hoppe, T., Schlenker, S., Ulrich, H.D., Mayer, T.U., and Jentsch, S. (1999). A novel ubiquitination factor, E4, is involved in multiubiquitin chain assembly. Cell *96*, 635–644.

Lai, E.C., Deblandre, G.A., Kintner, C., and Rubin, G.M. (2001). *Drosophila* neuralized is a ubiquitin ligase that promotes the internalization and degradation of delta. Dev. Cell *1*, 783–794.

Lee, T., and Luo, L. (1999). Mosaic analysis with a repressible cell marker for studies of gene function in neuronal morphogenesis. Neuron *22*, 451–461.

Lee, T., Lee, A., and Luo, L. (1999). Development of the *Drosophila* mushroom bodies: sequential generation of three distinct types of neurons from a neuroblast. Development *126*, 4065–4076.

Lee, T., Marticke, S., Sung, C., Robinow, S., and Luo, L. (2000a). Cell-autonomous requirement of the USP/EcR-B ecdysone receptor for mushroom body neuronal remodeling in *Drosophila*. Neuron *28*, 807–818.

Lee, T., Winter, C., Marticke, S.S., Lee, A., and Luo, L. (2000b). Essential roles of *Drosophila* RhoA in the regulation of neuroblast proliferation and dendritic but not axonal morphogenesis. Neuron *25*, 307–316.

Liu, Z., Steward, R., and Luo, L. (2000). *Drosophila* Lis1 is required for neuroblast proliferation, dendritic elaboration and axonal transport. Nat. Cell Biol. *2*, 776–783.

Mack, T.G., Reiner, M., Beirowski, B., Mi, W., Emanuelli, M., Wagner, D., Thomson, D., Gillingwater, T., Court, F., Conforti, L., et al. (2001). Wallerian degeneration of injured axons and synapses is delayed by a Ube4b/Nmnat chimeric gene. Nat. Neurosci. *4*, 1199–1206.

Miller, R.J., and Wilson, S.M. (2003). Neurological disease: UPS stops delivering! Trends Pharmacol. Sci. *24*, 18–23.

Moline, M.M., Southern, C., and Bejsovec, A. (1999). Directionality of wingless protein transport influences epidermal patterning in the *Drosophila* embryo. Development *126*, 4375–4384.

Nakamura, H., and O'Leary, D.D. (1989). Inaccuracies in initial growth and arborization of chick retinotectal axons followed by course corrections and axon remodeling to develop topographic order. J. Neurosci. *9*, 3776–3795.

O'Leary, D.D.M., and Koester, S.E. (1993). Development of projection neuron types, axon pathways, and patterned connections of the mammalian cortex. Neuron *10*, 991–1006.

Perry, V.H., Lunn, E.R., Brown, M.C., Cahusac, S., and Gordon, S. (1990). Evidence that the rate of Wallerian degeneration is controlled by a single autosomal dominant gene. Eur. J. Neurosci. *2*, 408–413.

Raff, M.C., Whitmore, A.V., and Finn, J.T. (2002). Axonal self-destruction and neurodegeneration. Science *296*, 868–871.

Rorth, P. (1996). A modular misexpression screen in *Drosophila* detecting tissue-specific phenotypes. Proc. Natl. Acad. Sci. USA *93*, 12418–12422.

Sanes, J.R., and Lichtman, J.W. (1999). Development of the vertebrate neuromuscular junction. Annu. Rev. Neurosci. *22*, 389–442.

Shih, S.C., Katzmann, D.J., Schnell, J.D., Sutanto, M., Emr, S.D., and Hicke, L. (2002). Epsins and Vps27p/Hrs contain ubiquitin-binding domains that function in receptor endocytosis. Nat. Cell Biol. *4*, 389–393.

Talbot, W.S., Swyryd, E.A., and Hogness, D.S. (1993). Drosophila tissues with different metamorphic responses to ecdysone express different ecdysone receptor isoforms. Cell *73*, 1323–1337.

Truman, J.W. (1990). Metamorphosis of the central nervous system of *Drosophila*. J. Neurobiol. *21*, 1072–1084.

Waller, A. (1850). Experiments on the section of glossopharyngeal and hypoglossal nerves of the frog and observations of the alternatives produced thereby in the structure of their primitive fibers. Phil Trans R Soc Lond *140*, 423–429.

Walsh, M.K., and Lichtman, J.W. (2003). In vivo time-lapse imaging of synaptic takeover associated with naturally occurring synapse elimination. Neuron *37*, 67–73.

Wan, H.I., DiAntonio, A., Fetter, R.D., Bergstrom, K., Strauss, R., and Goodman, C.S. (2000). Highwire regulates synaptic growth in *Drosophila*. Neuron *26*, 313–329.

Weimann, J.M., Zhang, Y.A., Levin, M.E., Devine, W.P., Brulet, P., and McConnell, S.K. (1999). Cortical neurons require Otx1 for the refinement of exuberant axonal projections to subcortical targets. Neuron *24*, 819–831.

Weissman, A.M. (2001). Themes and variations on ubiquitylation. Nat. Rev. Mol. Cell Biol. *2*, 169–178.

White, K., Grether, M.E., Abrams, J.M., Young, L., Farrell, K., and Steller, H. (1994). Genetic control of programmed cell death in *Drosophila*. Science *264*, 677–683.

Winter, C.G., Wang, B., Ballew, A., Royou, A., Karess, R., Axelrod, J.D., and Luo, L. (2001). *Drosophila* Rho-associated kinase (Drok) links Frizzled-mediated planar cell polarity signaling to the actin cytoskeleton. Cell *105*, 81–91.

Zheng, X., Wang, J., Haerry, T.E., Wu, A.Y., Martin, J., O'Connor, M.B., Lee, C.H., and Lee, T. (2003). TGF-beta signaling activates steroid hormone receptor expression during neuronal remodeling in the *Drosophila* brain. Cell *112*, 303–315.

Zhu, H., Kavsak, P., Abdollah, S., Wrana, J.L., and Thomsen, G.H. (1999). A SMAD ubiquitin ligase targets the BMP pathway and affects embryonic pattern formation. Nature *400*, 687–693.